

# Multibody Dynamic Simulations of Unbalance Induced Vibration and Transfer Characteristics of Inner and Outer Dual-rotor System in Aero-engine

Pingping Ma<sup>1,2</sup> Hao Zhang<sup>1,2</sup> Jingyu Zhang<sup>1</sup> Qingkai Han<sup>1,2\*</sup>

<sup>1</sup> School of Mechanical Engineering, Dalian University of Technology, Dalian, PR China

<sup>2</sup> Collaborative Innovation Center of Major Machine Manufacturing in Liaoning, Dalian University of Technology, Dalian, PR China

**Abstract:** An unbalance vibration simulation method of dual-rotor system is proposed in this paper based on multi-body dynamic. Based on the theories of dual-rotor system dynamic, together with the unbalanced simulation method, a multi-body dynamic model of the aero-engine dual-rotor system is built on the software platform of ADMAS. The modal analyses of the first two natural frequencies and mode shapes are compared in order to check the dynamic similarity of them, for both multi-body dynamics model and the analytical results. Multi-plane and multi-phase unbalance vibration of the dual-rotor system is simulated with intermediate bearing coupling effect considered. The unbalance value is extracted based on sampling principle of Monte Carlo. The numerically simulated time-domain responses, the frequency spectra and the shaft-center trajectories are plotted and compared under the above varied operating conditions. Most important of all, the vibration coupling and transfer among the high-pressure rotor and the low-pressure rotor are revealed as well. Apart from that, the relationship between dual-rotor vibration response and unbalanced force and the couple which produced by the unbalance of low pressure turbine disc and the low pressure compressor disc is summarized in this paper. The study of multi-plane and multi-phase unbalance vibration response and coupling characteristics of inner and outer dual-rotor system provides a verification method for dynamic balance research on the aircraft engine dual-rotor system.

**Keywords:** Dual-rotor; Multi-body dynamic; Coupling characteristics; Multi-plane and multi-phase unbalance; Numerically simulate;

## 1 Introduction

According to statistics, more than 70% of the aero engine fault is derived from the vibration<sup>[1]</sup>, and the unbalance of the rotor system is the main factor causes the vibration of the aero engine, which is the most basic and most common form of excitation in the operation of the rotor system. It is unavoidable for both the high and low pressure rotors in the motion of dual-rotor system. The unbalanced excitation and the vibration of the dual-rotor system become more complicated because of the medium bearing which connects the inner rotor and outer rotor.

Although there are lots of researches on the unbalanced vibration of rotor, the transfer law of unbalance vibration is not clear and the dynamic balance problem of dual-rotor system is not solved. It is urgent to carry out the research on the unbalanced vibration of the rotor system. Gupta et al.<sup>[2]</sup> clearly show the presence of cross-excitation between the inner and outer shafts through experimental results. Jiang Yunfan et al.<sup>[3]</sup> studied the dynamic characteristics of the double rotors with the co-rotating and the counter-rotating. It is found that the unbalance response of counter-rotating dual-rotor is more obvious than the co-rotating dual-rotor under the same unbalance mass. Jinji Gao et al.<sup>[4]</sup> established dynamic finite element models of single-span-rotor and coupled-rotor system, and the dynamic response of the rotor residual unbalance is obtained by numerical method. Yang Yang et al.<sup>[5]</sup> analyzed the vibration response of a dual-disc rotor system with multi-unbalances, multi-fixed-point rubbing faults. It was found that the response of the rotor system is very complicated, when the direction of the first

---

\* Corresponding author (hanqingkai@dlut.edu.cn)

unbalance force is the same as that of the second unbalance force. When the directions of two unbalance forces are exactly opposite, the response of the rotor system is relatively simple and the vibration amplitude decreases obviously. What's more, the motions of the rotor system are more sensitive to the parameters of the compressor disc, while Those of the turbine disc can only affect the motions of the rotor system slightly. The unbalance and dynamic balance of rotor are also studied in document [6-10], in which [10] studied the vibration response of multi-rotor system with multiple disks through theoretical analysis.

ADAMS is based on computational multi-body dynamics in theory, including many professional modules, which can be used to establish the complex kinematics and dynamics of mechanical systems. So ADAMS can implement the simulation of kinematics and dynamics of the system in actual condition [11]. Qingkai Han et al. [12] developed a rigid-flexible multi-body model for a dual-rotor system with local rub-impacts with Adams. On the basis of the unbalanced theory, the dynamic model of the dual-rotor system in aero engine is carried out with the help of ADMAS, and the unbalance simulation method is introduced. Multi-plane and multi-phase unbalance vibration of the dual-rotor system is simulated with intermediate bearing coupling effect considered. The unbalance value is extracted based on sampling principle of Monte Carlo. The frequency domain and the axis trajectory of the unbalanced vibration of the dual-rotor system are obtained. Apart from that, the relationship between dual-rotor vibration response and unbalanced force and the couple which produced by the unbalance of low pressure turbine disc and the low pressure compressor disc is summarized in this paper.

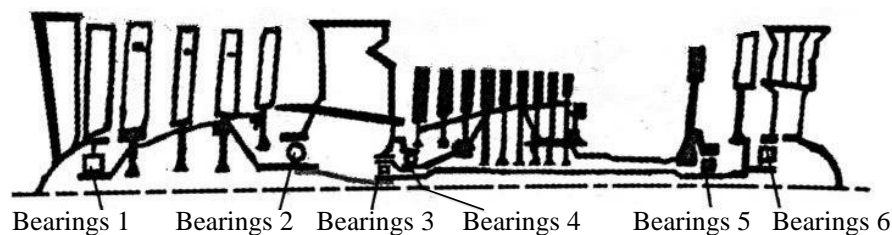
## 2 Dynamic model of the inner and outer dual-rotor system

The structure of dual-rotor system of aero engine is complicated which mainly composed of rotating shaft, supporting structure and disc. Therefore, it is necessary to simplify the dual-rotor system and built an appropriate finite element model adapt to the computing power. This paper have analyzed the structural and dynamic characteristics of a certain aero engine real rotor system, and obtained the simplified model of the dual-rotor system based on the principle of structural similarity and of dynamic similarity.

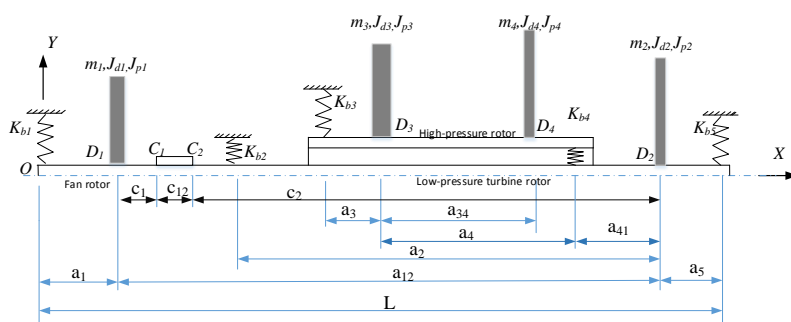
### 2.1 Establishment of a simplified model of dual-rotor system based on similarity principle

Figure 1(a) shows the structure of a dual-rotor system for a certain aero engine. The main components of the dual-rotor system are fan rotor, low-pressure turbine rotor, high pressure rotor, discs, bearings and gear coupling. The low-pressure rotor consists of three supportings, four stage fan discs and one stage turbine disc. The high pressure rotor consists of two supportings, nine stage compressor discs, one stage seal disc and one stage high pressure turbine disc. The low pressure rotor connects with the high pressure rotor through an intermediate bearing make up the dual-rotor. The dynamic characteristics of the dual-rotor system are influenced by the high and low pressure rotor, and have some unique vibration characteristics.

The shaft of simplified model rotor is obtained by parameterized and regularization the shaft of the prototype. According to the equivalent of Mass and Moment of Inertia, fan disc (LPC), low pressure turbine disc(LPT), high pressure compressor disc (HPC) and high pressure turbine disc (HPT) of the prototype are simplified as one wheel disc respectively. The supporting 2 and 3 are simplified into a support, which stiffness is the series stiffness of the two, and the simplified four-disc-five-fulcrum model is shown in Figure 1(b).



(a) The schematic diagram of the aero engine rotor



(b) The simplified dynamic model of dual rotor system

**Fig. 1.** The simplified dynamic model of the aero engine dual-rotor

## 2.2 Establishment of the dual rotor dynamic equations

The system analytic model is established by using the Lagrange equation as follows.

$$\frac{d}{dt} \frac{\partial T}{\partial \dot{q}_j} - \frac{\partial T}{\partial q_j} + \frac{\partial U}{\partial q_j} + \frac{\partial D}{\partial \dot{q}_j} = Q_j(t), \quad j = 1, 2, 3 \dots \quad (1)$$

Where,  $q_j$  and  $\dot{q}_j$  are generalized coordinates and generalized velocities respectively.  $T$  and  $U$  are the kinetic energy and potential energy of the system respectively.  $D$  is the energy dissipation function of the system.  $Q_j(t)$  is the generalized external excitation force. If the work done by some exciting force has been expressed as the kinetic energy and potential energy form of the vibration system, or the form of energy dissipation function, then these exciting forces are no longer considered on the right side of the equation. In this rotor system, the influence of energy dissipation function  $D$  is neglected. Function (1) can be written as

$$\frac{d}{dt} \frac{\partial T}{\partial \dot{q}_j} - \frac{\partial T}{\partial q_j} + \frac{\partial U}{\partial q_j} = Q_j(t), \quad j = 1, 2, 3 \dots \quad (2)$$

Considering the motion equation of the rotor, and ignoring the external excitation. The differential equations of the system motion are derived and arranged as follows.

$$\begin{aligned} m_1 \ddot{y}_1 + k_{cy} (\theta_{z1} c_1 + \theta_{z2} c_2 + y_1 - y_2) + k_{b1y} (y_1 - a_1 \theta_{z1}) &= 0 \\ m_1 \ddot{z}_1 + k_{cz} (-\theta_{y1} c_1 - \theta_{y2} c_2 + z_1 - z_2) + k_{b1z} (z_1 + a_1 \theta_{y1}) &= 0 \\ J_{d1} \ddot{\theta}_{y1} + J_{p1} \Omega_1 \dot{\theta}_{z1} + k_{cz} \theta_{y1} c_1^2 - k_{cz} (-\theta_{y2} c_2 + z_1 - z_2) c_1 \\ + (k_{b1z} a_1^2 + k_{c\theta y}) \theta_{y1} + k_{b1z} a_1 z_1 - k_{c\theta y} \theta_{y2} &= 0 \\ J_{d1} \ddot{\theta}_{z1} - J_{p1} \Omega_1 \dot{\theta}_{y1} + k_{cy} c_1^2 \theta_{z1} + k_{cy} (\theta_{z2} c_2 + y_1 - y_2) c_1 \\ + (k_{b1y} a_1^2 + k_{c\theta z}) \theta_{z1} - k_{b1y} a_1 y_1 - k_{c\theta z} \theta_{z2} &= 0 \\ m_2 \ddot{y}_2 + (-k_{cy} c_2 - k_{b2y} a_2 - k_{b4y} a_{41} + k_{b5y} a_5) \theta_{z2} + k_{b4y} (-\theta_{z3} a_4 + y_2 - y_3) \\ + k_{cy} (-\theta_{z1} c_1 - y_1 + y_2) + (k_{b2y} + k_{b5y}) y_2 &= 0 \end{aligned}$$

$$\begin{aligned}
 & m_2 \ddot{z}_2 + (k_{cz} c_2 + k_{b2z} a_2 + k_{b4z} a_{41} - k_{b5z} a_5) \theta_{y2} + k_{b4z} (\theta_{y3} a_4 + z_2 - z_3) \\
 & + k_{cz} (\theta_{y1} c_1 - z_1 + z_2) + (k_{b2z} + k_{b5z}) z_2 = 0 \\
 & J_{d2} \ddot{\theta}_{y2} + J_{p2} \Omega_1 \dot{\theta}_{z2} + (k_{cz} c_2^2 + k_{b2z} a_2^2 + k_{b4z} a_{41}^2 + k_{b5z} a_5^2 + k_{c\theta y} + q_{b4\theta y}) \theta_{y2} \\
 & + k_{b4z} (\theta_{y3} a_4 + z_2 - z_3) a_{41} - k_{cz} (-\theta_{y1} c_1 + z_1 - z_2) c_2 + (k_{b2z} a_2 - k_{b5z} a_5) z_2 \\
 & - k_{c\theta y} \theta_{y1} - k_{b4\theta y} \theta_{y3} = 0 \\
 & J_{d2} \ddot{\theta}_{z2} - J_{p2} \Omega_1 \ddot{\theta}_{y2} + (k_{cy} c_2^2 + k_{b2y} a_2^2 + k_{b4y} a_{41}^2 + k_{b5y} a_5^2 + k_{c\theta z} + k_{b4\theta z}) \theta_{z2} \\
 & + k_{b4y} (\theta_{z3} a_4 - y_2 + y_3) a_{41} + k_{cy} (\theta_{z1} c_1 + y_1 - y_2) c_2 + (-k_{b2y} a_2 + k_{b5y} a_5) y_2 \\
 & - k_{c\theta z} \theta_{z1} - k_{b4\theta z} \theta_{z3} = 0 \\
 & (m_3 + m_4) \ddot{y}_3 + m_4 a_{34} \ddot{\theta}_{z3} + k_{b4y} (\theta_{z2} a_{41} + \theta_{z3} a_4 - y_2 + y_3) - k_{b3y} \theta_{z3} a_3 + k_{b3y} y_3 = 0 \\
 & (m_3 + m_4) \ddot{z}_3 - m_4 a_{34} \ddot{\theta}_{y3} + k_{b4z} (-\theta_{y2} a_{41} - \theta_{y3} a_4 - z_2 + z_3) + k_{b3z} \theta_{y3} a_3 + k_{b3z} z_3 = 0 \\
 & (m_4 a_{34}^2 + J_{d3} + J_{d4}) \ddot{\theta}_{y3} - m_4 a_{34} \ddot{z}_3 + (J_{p3} + J_{p4}) \Omega_3 \dot{\theta}_{z3} + a_4^2 k_{b4z} \theta_{y3} \\
 & + k_{b4z} (\theta_{y2} a_{41} + z_2 - z_3) a_4 + (k_{b3z} a_3^2 + k_{b4\theta y}) \theta_{y3} + k_{b3z} a_3 z_3 - k_{b4\theta y} \theta_{y2} = 0 \\
 & (m_4 a_{34}^2 + J_{d3} + J_{d4}) \ddot{\theta}_{z3} + m_4 a_{34} \ddot{y}_3 - \Omega_3 (J_{p3} + J_{p4}) \dot{\theta}_{y3} + k_{b4y} a_4^2 \theta_{z3} \\
 & + k_{b4y} (\theta_{z2} a_{41} - y_2 + y_3) a_4 + (k_{b3y} a_3^2 + k_{b4\theta z}) \theta_{z3} - k_{b3y} a_3 y_3 - k_{b4\theta z} \theta_{z2} = 0
 \end{aligned} \tag{3}$$

### 2.3 Establishment and verification of multi-body dynamics model for dual-rotor system

To study the calculation method of ADAMS theory, first of all, we should establish the dynamic equation of the system. In this process, the selection of the coordinate system is particularly important, especially the generalized coordinates. In ADAMS, the general coordinates of the system are expressed by the Descartes coordinates which are associated by the rigid body centroid and the Euler angles which describe the phase space of rigid body. The specific expressions are  $q_i = [x, y, z, \psi, \theta, \varphi]_i^T$ . From the above expression, the number of the coordinates required for each rigid body is six. Based on Lagrange Multiplier, the dynamic equations of multi-rigid body system are derived as follows.

$$\frac{d}{dt} \left( \frac{\partial B}{\partial \dot{q}} \right)^T - \left( \frac{\partial B}{\partial q} \right)^T + S_q^T \rho + V_q^T \mu = Q \tag{4}$$

$$\varphi(q, t) = 0, \quad \theta(q, \dot{q}, t) = 0 \tag{5}$$

Where B represents the kinetic energy of system; q,  $\dot{q}$ ,  $\rho$ ,  $V_q$ , Q are the generalized coordinate matrix, displacement constraint matrix, Lagrangian multiplier matrix corresponding to the complete constraint, velocity constraint matrix, Lagrangian multiplier matrix corresponding to the complete constraint, velocity constraint matrix, Lagrangian multiplier matrix corresponding to the nonholonomic constraint and generalized force matrix.  $\varphi(q, t) = 0$  is a holonomic constraint equation, and  $\theta(q, \dot{q}, t)$  is a nonholonomic constraint equation.

When the dual-rotor system dynamic model is built in Adams, the elastic support is simulated by the spring damping element, which stiffness parameters are set to some values,  $K_1=K_4=k_6=3.3e7N/m$ ,  $k_{2/3}=K_5=2.5e8N/m$ . The fan shaft and the low pressure turbine shaft are connect by the coupling and which the stiffness is equal to  $1e8N/m(Kc)$ . To improve the calculation efficiency, the coupling is simplified into axis in ADAMS as shown in Figure 2.

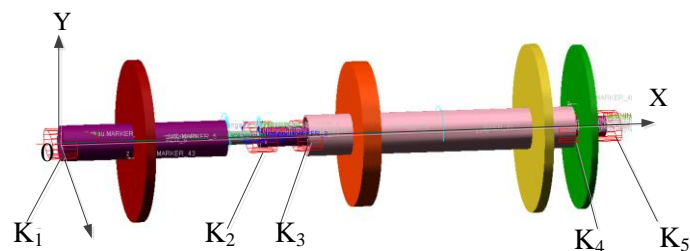


**Fig. 2.** Multi-body dynamic model of dual-rotor based on Adams

In order to make the speed rise slowly, avoid too much impact, the drive function of the shaft use step function. The inner and outer rotor speed sets  $N_1=8800\text{r/min}$ ,  $N_2=12000\text{r/min}$  as shown in Figure 3.

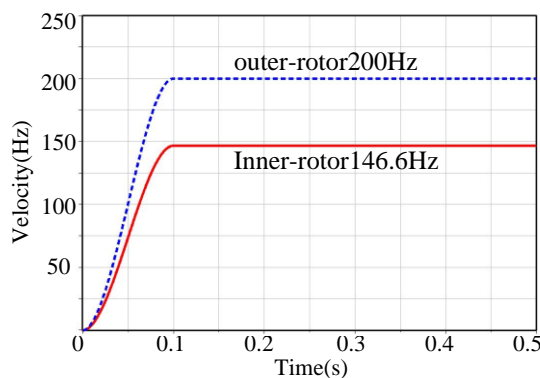


**Fig. 3.** Rotating speeds of inner and outer rotor

The modal analyses of the first two natural frequencies and mode shapes are compared in order to check the dynamic similarity of them, as shown in Table 1, for both multi-body dynamics model and the analytical results. It can be clearly seen that, the first two order forms are the same and the frequency difference is small. The first order natural frequency of the Adams calculation is smaller than that of the analytical solution, may caused by the simplify of the coupling.

**Table 1.** Dual-rotor Mode comparison of simulation and analysis

Order	Based on Simulation	Based on analytic theory
1st	<p>72Hz</p>	<p>79Hz</p> <p>— Inner-rotor - - - outer-rotor △ Supporting</p>
2st	<p>94Hz</p>	<p>95Hz</p> <p>— Inner-rotor - - - outer-rotor △ Supporting</p>

### 3 Unbalanced vibration response characteristics of dual-rotor system

The unbalance of the dual-rotor system is simulated by the additional mass blocks on LPC, LPT, HPC and HPT. Setting the positive direction of the Y axis is 0 phase and the phase difference  $\theta$  changes clockwise with a range of  $0^\circ$  to  $360^\circ$  in the YZ plane as shown in Figure 4.

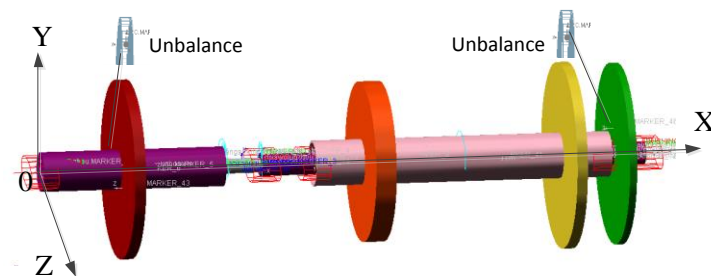


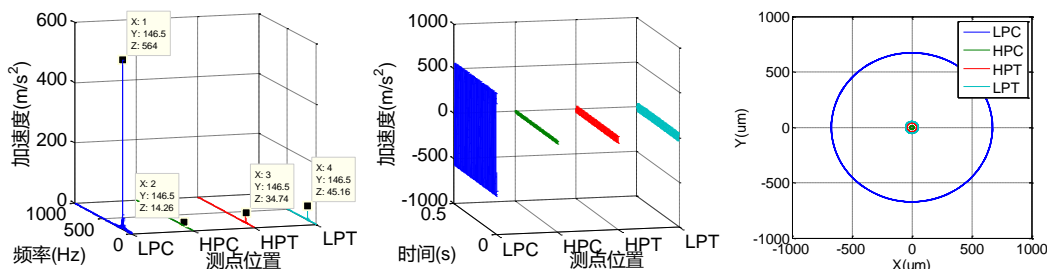
Fig. 4. The simulation model for unbalance vibration of dual-rotor based on Adams

### 3.1 Unbalanced vibration response characteristics of dual-rotor system caused by one disc

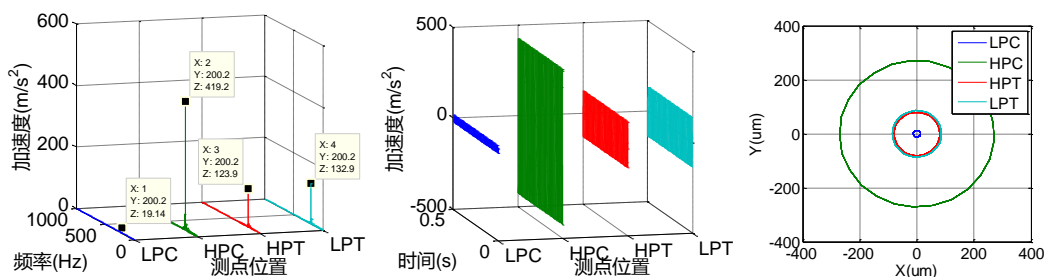
The influence of unbalanced position on vibration response of dual-rotor is extracted from the following 4 working conditions. The orbit of four discs center and the frequency spectra of speed and acceleration are obtained through the simulation in figure 5.

Table 2. Unbalances parameters of disc

case	LPC		HPC		HPT		LPT	
	m*e	phase	m*e	phase	m*e	phase	m*e	phase
1	200	0						
2			200	0				
3					200	0		
4							200	0



(a) LPC unbalance



(b) HPC unbalance

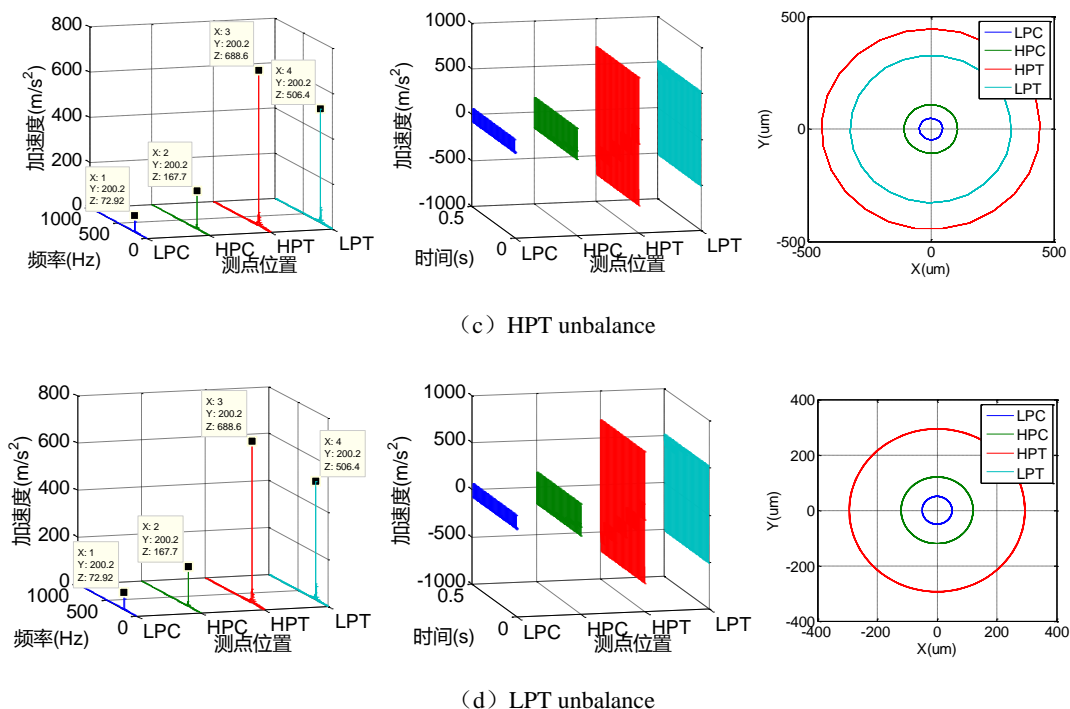


Fig. 5. Case I -IV, unbalance vibration response of dual-rotor

Through the above four unbalance settings, the following conclusions are obtained. The unbalance vibration response spectrum main component is N1 which induced by LPC and LPT. While HPC and HPT unbalance cause N2 is the mainly frequency in the vibration response spectrum of dual-rotor.

LPC and HPC unbalance vibration in the transfer path LPC-LPT-HPT-HPC and HPC-HPT-LPT-LPC decrease step by step respectively. The unbalance transfer rate HPT-LPT is greater than HPT-HPC. Vibration of HPT is most large while LPC is the smallest among the four discs, when LPT unbalance.

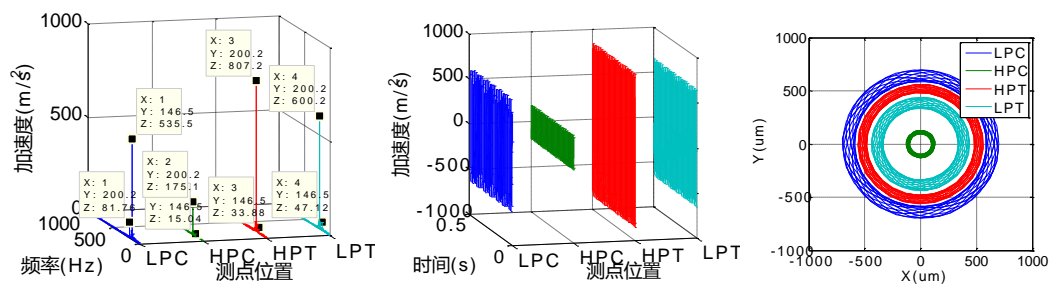
### 3.2 Multi-plane and multi-phase unbalance vibration transformation and coupling characteristics of dual-rotor system

The vibration response of dual-rotor not only related to the unbalance position, but also unbalance phase. In order to explore the effect of the size and phase of different unbalances on the vibration of dual-rotor system, it is necessary to find a way to obtain the size and distribution of the unbalance value of the rotor. In this paper, 8 groups of unbalance distributions are extracted from the state sampling method based on Monte-Carlo, as shown in Table 3. By analyzing the vibration responses of the dual-rotor under the 8 cases shown in Table 3, the axis trajectories and the frequency spectra of speed and acceleration at each measuring point under different working conditions are obtained as shown in Fig. 6.

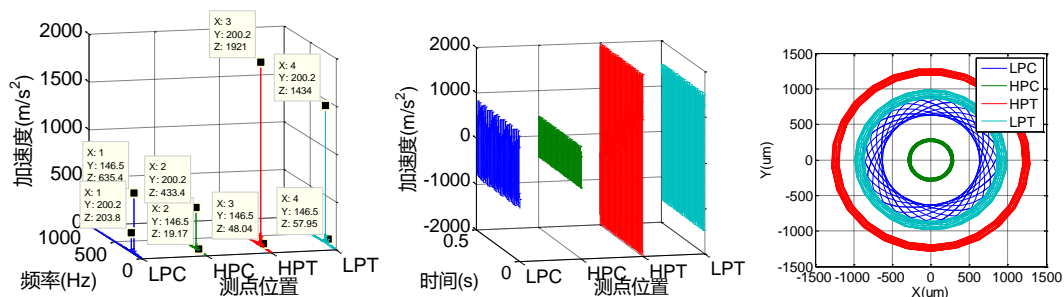
Table 3. Multi-plane and multi-phase unbalance parameters

case	LPC		HPC		HPT		LPT	
	m*e	phase	m*e	phase	m*e	phase	m*e	phase
1	197	244	86	272	212	267	10	141
2	208	99	159	16	285	34	10	296
3	56	158	245	137	134	275	194	286
4	197	255	81	271	36	99	150	244
5	225	345	128	122	152	210	210	80
6	45	320	129	345	252	197	76	50
7	59	293	126	87	185	334	142	126

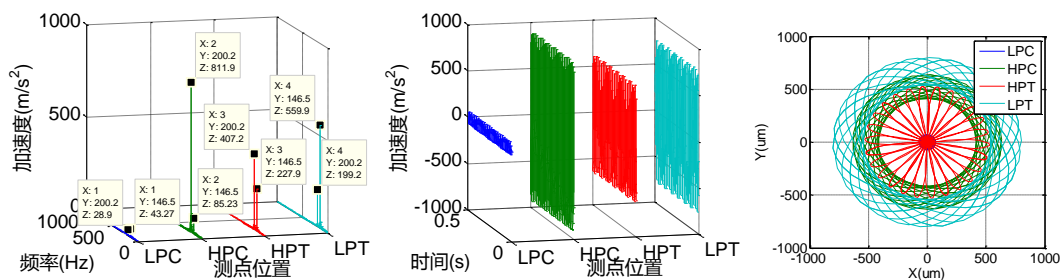
8	275	126	143	299	227	210	226	198
---	-----	-----	-----	-----	-----	-----	-----	-----



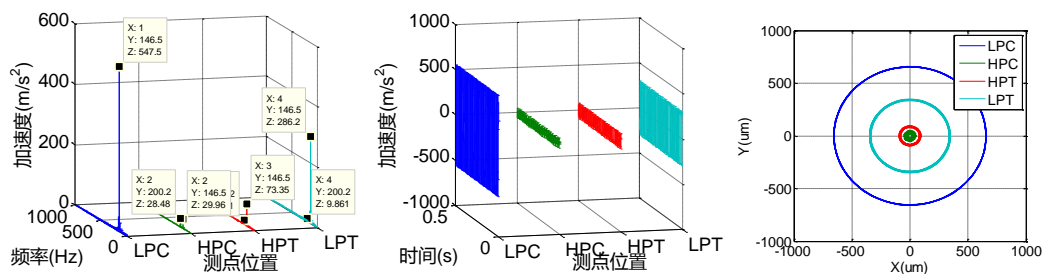
(a) Case I



(b) Case II



(c) Case III



(d) Case IV



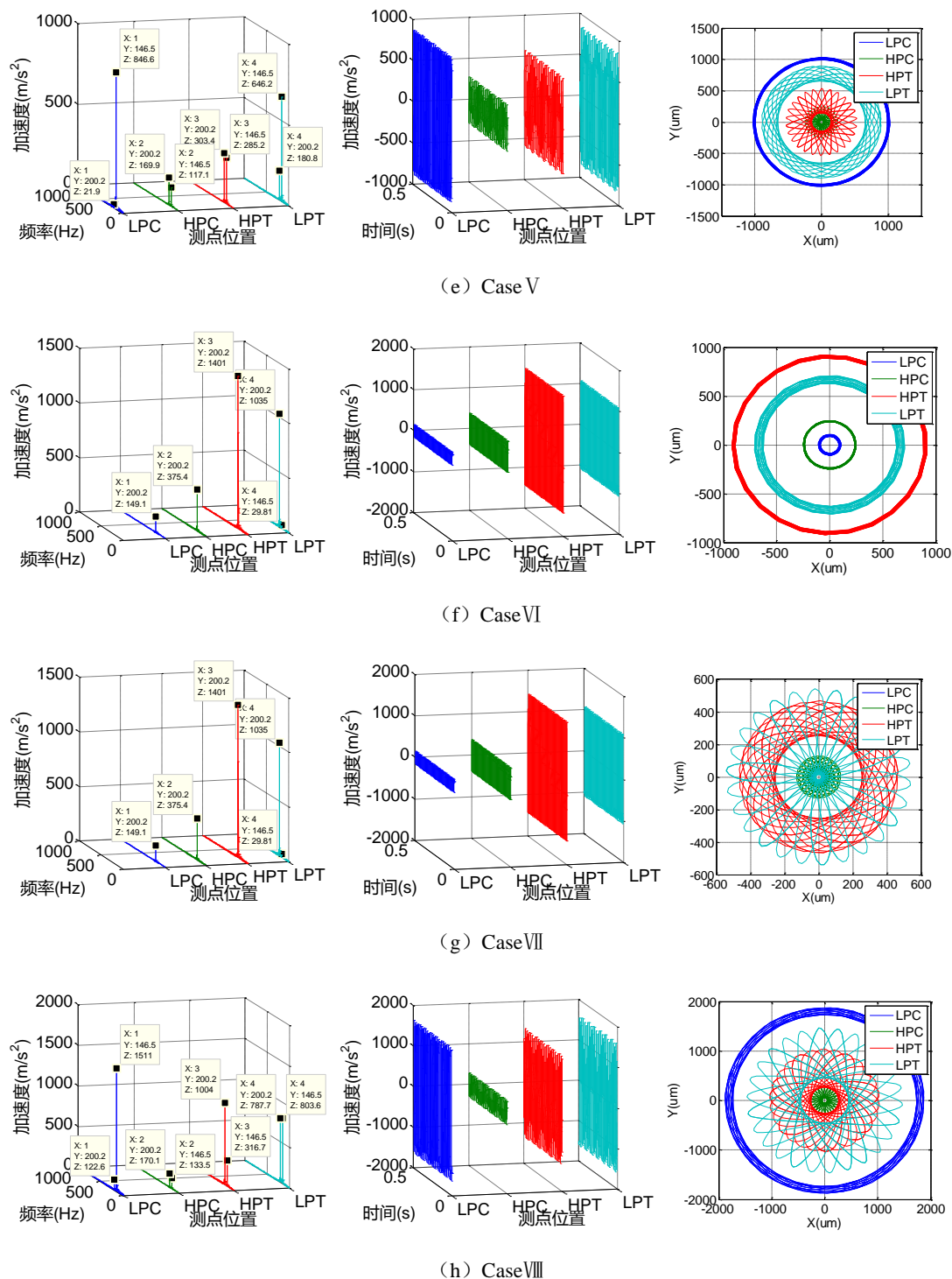


Fig. 6. Case I -VIII, unbalance vibration response of dual-rotor

Compared with the vibration response of dual-rotor in Fig.6, can be see that if the unbalance value very small and the response amplitude large of LPT, the vibration is caused by HPT, the spectrum of LPT is dominated by N2. The effect of LPT unbalance on HPT vibration response is larger than that of HPC unbalance .The vibration transfer ratio of HPT- LPT is greater than HPT-HPC. When the two values of N1 and N2 in the frequency spectrum are equal, the axis trajectory of the disc is petal shape, the more single the frequency in the spectrum, the more regular the axis trajectory is.

#### 4 The influence of unbalanced force and the couple on the vibration response of dual-rotor

In this section, the unbalance phase of discs and the coupling relationship between them are studied.

To use the method of adjust the relative phase between the rotor to reduce or even eliminate the shaft unbalance.

According to the principle of force translation and synthesis, the unbalance force produced by LPC and the LPT is synthesized at the 5# intermediate bearing. The resultant forces and moments generated by unbalance are expressed as follows:

$$F = \sqrt{F_1^2 + F_2^2 + 2F_1F_2 \cos \alpha} \tag{6}$$

Where  $\alpha$  is the angle of the unbalance force produced for the LPC and the LPT,  $F_1 = m_1e_1w^2$ ,  $F_2 = m_2e_2w^2$ .

$$M_y = -F_1 \sin \theta_1 L_1 + F_2 \sin \theta_2 L_2 \tag{7}$$

$$M_z = -F_1 \cos \theta_1 L_1 + F_2 \cos \theta_2 L_2 \tag{8}$$

Among them,  $L_1$  and  $L_2$  are the distance from the LPT and LPT to the 5# supporting respectively.

Keeping the unbalance is 100g.mm of LPC and LPT,  $\theta_2 = 0^\circ$ ,  $\theta_1$  from 0 to 360 degrees by uniform sampling as shown in Figure 7. The vibration displacement amplitudes resultant curves of the LPC and LPT under different phase difference as shown in Fig. 8.

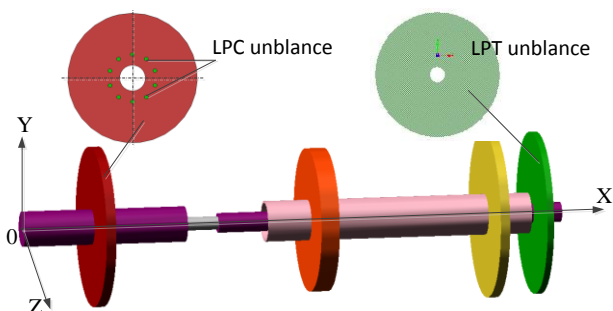


Fig. 7. Unbalance setting of LPC and LPT

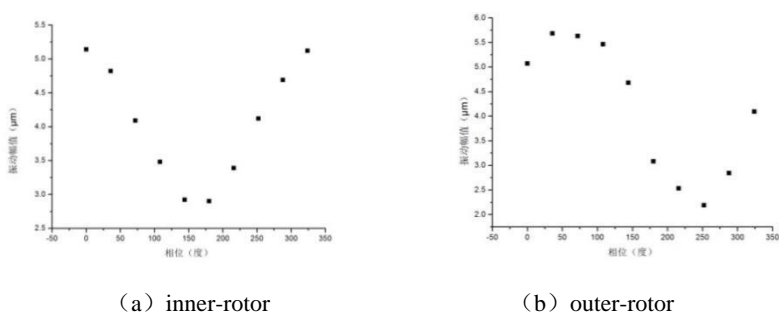


Fig. 8. Inner and outer rotor vibration fitting curves variety from phase difference

According to formula (1),  $\theta_2 = 0$  and  $F_1 = F_2$  can be obtained the following formula.

$$F = \sqrt{2}F_1\sqrt{1 + \cos \theta_1} \tag{9}$$

$$M = F_1\sqrt{L_1^2 + L_2^2 - 2L_1L_2 \cos \theta_1} \tag{10}$$

The change curve of  $F-\theta_1$  and  $M-\theta_1$  is shown in Figure 9.

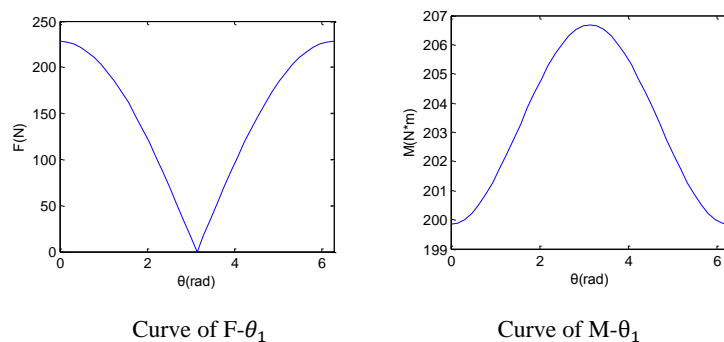


**Fig. 8.** F and M fitting curves variety from phase difference

In this subsection, a variable  $\theta_1$  is defined to describe the phase difference between two unbalance forces cause by LPC and LPT. Comparing the results of theory with multi-body dynamics simulation, it can be see that outer-rotor vibration is mainly affected by unbalance torque because of the curve of outer-rotor consistent with the torque changing produced by unbalances, and the phase difference is 90 degrees. Inner-rotor vibration is mainly affected by unbalance force because of the curve of inner-rotor have the same change trend with the force produced by unbalances. It shows that the vibration of the low pressure rotor is mainly influenced by the unbalance force when the LPC and LPT are unbalance. It lays the foundation for studying the influence of multi-disc and multi-phase random unbalance force and couple on rotor vibration, and provides theoretical basis for monitoring and control of dynamic balance.

## 5 Conclusions

In this paper, an unbalance vibration simulation method of dual-rotor system is proposed based on multi-body dynamics. Multi-plane and multi-phase unbalance vibration of the dual-rotor system is simulated with intermediate bearing coupling effect considered. The simulation results are verified by the analytical method. The analysis results are shown below.

1) The unbalanced vibration response of the dual-rotor is not only related to the size of the unbalance, but also with the position of unbalance. N1 and N2 is the main frequency of the unbalanced response of dual-rotor system.

2) The ratio of the unbalanced transmission of the high pressure turbine disc to the low pressure turbine disc is greater than that to the high pressure compressor disc. If the unbalance of the low pressure turbine disc is small and the response amplitude is large, it is caused by the unbalance of the high pressure turbine disc, and N2 is mainly frequency of the response.

3) In the process of inner and outer rotor unbalance response, the high and low pressure turbine disc are most sensitive, and the low-pressure compressor disc is the most stable.

4) when the low pressure compressor and the low pressure turbine disc have different phase unbalance, the vibration of the inner and outer rotor are mainly affected by the unbalanced torque and the unbalance force respectively.

The study of unbalanced vibration response and coupling characteristics of dual-rotor system in this paper, preliminarily revealed the unbalance vibration law of inner and outer rotor. Providing the basis for the unbalance vibration diagnosis, evolution and monitor. Adding a verification method for aero engine rotor unbalance theory.

## References

- 1 Y.S. Chen, H. Zhang, Research progress and prospect of aero-engine dynamics, *Acta Aeronautica ET Astronautica Sinica*, 32 (2011)1371-1391.
- 2 A.K. Guptak, D. Guptak, Unbalance Response of a dual rotor system: theory and experiment, *Journal of Vibration & Acoustics*, 115 (1993) 427-435.
- 3 Y.F. Jiang, M.F. Liao, Y.Q. Liu, Dynamic characteristics of co-rotating/counter-rotating dual-rotor system, *Journal of Aerospace Power*, 28 (2013) 2771-2779.
- 4 J.J. Gao, H.Y. Miu, H. Xu, Optimal coupling of multi rotor shafting and finite element analysis of its unbalanced response, *Journal of Vibration and Shock*, 24 (2005) 1-4.

- 5 Y. Yang, D.Q. Cao, T.H. Yu, D.Y. Wang, C.G. Li, Response analysis of a dual-disc rotor system with multi-unbalances–multi-fixed-point rubbing faults, *Nonlinear Dynamic*, 87 (2017) 109-125.
- 6 G. Sudhakar, A.S. Sekhar, Identification of unbalance in a rotor bearing system, *Journal of Sound & Vibration*, 330 (2011) 2299-2313.
- 7 R. Tiwari, V. Chakravarthy, Simultaneous identification of residual unbalances and bearing dynamic parameters from impulse responses of rotor–bearing systems, *Mechanical Systems & Signal Processing*, 20 (2006) 1590-1614.
- 8 S. Liu, A modified low-speed balancing method for flexible rotors based on holospectrum, *Mechanical Systems & Signal Processing*, 21 (2006) 348-364.
- 9 S. Liu, A New Balancing Method for Flexible Rotors Based on Neuro-fuzzy System and Information Fusion, *Lecture Notes in Computer Science*, 36 (2005) 757-760.
- 10 G.S. Wei, H. Zhang, P.P. Ma, Q.K. Han, Multi-plane and multi-phase unbalance vibration response and coupling characteristics of inner and outer dual rotor system.
- 11 S. Xue, X.U. Long, Y. Zhao, et al., Comparative analysis of Hertz contact simulation based on Adams and RecurDyn, *Journal of Changchun University of Science & Technology*, 39 (2016) 73-77.
- 12 Q.K. Han, H.T. Luo, B.C. Wen, Simulations of a dual-rotor system with local rub-impacts based on rigid-flexible multi-body model, *Key Engineering Materials*, (2009) 677-682.